

## Scaling behavior near a valence instability: The magnetic susceptibility of $\text{CeIn}_{3-x}\text{Sn}_x$

Jon Lawrence

*Department of Physics, University of California, Irvine, California 92717*

(Received 22 March 1979)

Significant deviations from Vegard's law in  $\text{CeIn}_{3-x}\text{Sn}_x$  suggest a continuous valence transition from trivalence for  $x < 2.3$  to a small amount of mixed-valence character for  $x > 2.3$ . Results for the magnetic susceptibility  $\chi(x; T)$  in the range 2–340 K (with the background  $d$ -orbital contribution estimated from the susceptibility of  $\text{LaIn}_{3-x}\text{Sn}_x$  and subtracted off) exhibit several significant features: (i) For  $0.8 < x < 3.0$  the effective moment  $\mu^2 = T\chi/C$  is, to within a few percent, a function of a single scaled variable  $\mu^2(T, x) = \mu^2(T/T_{\text{sf}}(x))$ . This is interpreted as single-energy-scale characteristic-energy behavior, where  $kT_{\text{sf}}$  is a characteristic energy for spin fluctuations which varies from 50 to 200 K. (ii)  $T_{\text{sf}}(x)$  oscillates with  $x$  proportionally to the conduction-electron density of states  $N(\epsilon_F; x)$  (deduced from the electronic properties of  $\text{LaIn}_{3-x}\text{Sn}_x$ ); this provides strong evidence that the spin fluctuations arise from interactions of the  $4f$  spins with conduction electrons. (iii) The indium-rich alloys order magnetically at low temperature in some version of antiferromagnetism. The phase diagram, in which there is a  $T = 0$  phase transition from the antiferromagnetic ground state to a nonmagnetic trivalent spin-fluctuation ground state, is presented. This transition may correlate with an increase in the coupling  $\mathcal{J}\vec{\sigma}\cdot\vec{S}_f$  of conduction electrons to the  $4f$  spins, as recently proposed. The scaling behavior breaks down in the vicinity of the ordered phase as the magnetic interactions stabilize the low-temperature moment.

### I. INTRODUCTION

Valence instabilities<sup>1,2</sup> occur in cerium-based materials when the  $4f$  level  $E_f$  is moved to the Fermi level  $\epsilon_F$  by application of pressure or alloying. The following summarizes the behavior: When  $E_f$  is sufficiently far below  $\epsilon_F$  the metal will be trivalent and the ground state magnetically ordered. When  $E_f$  is not as far below  $\epsilon_F$  spin fluctuations (virtual valence fluctuations) will compete with the magnetic interaction, decreasing the moment. This may occur in  $\text{CeAl}_2$ .<sup>1</sup> As  $E_f$  approaches closer to  $\epsilon_F$  a situation is plausible where the metal, while still trivalent, has a nonmagnetic ground state: the spin fluctuations overcome the interaction. This would appear to hold in  $\text{CeAl}_3$ .<sup>1</sup> When  $\epsilon_F - E_f$  is comparable to the width of the hybridized  $4f$  level, the valence will become nonintegral, and valence fluctuations will play an increasingly important role; an example of this latter behavior would be  $\text{CePd}_3$ .<sup>3</sup> Finally, when the level is sufficiently far above  $\epsilon_F$  the metal will be tetravalent, as has been argued concerning  $\text{CeRh}_3$ .<sup>3</sup>

The results presented below concerning the magnetic behavior of the intermetallic alloy  $\text{CeIn}_{3-x}\text{Sn}_x$  seem to indicate that the above given sequence (magnetic ordering—trivalent spin-fluctuation behavior—intermediate valence) can be attained experimentally. In this system there is a valence transition with increasing concentration  $x$ .  $\text{CeIn}_3$  is

trivalent<sup>4</sup> and magnetically orders (at 10 K) but shows spin-fluctuation effects in the form of a large negative Curie-Weiss parameter<sup>5</sup> and a resistance minimum.<sup>6</sup>  $\text{CeSn}_3$  exhibits an anomalous lattice constant<sup>4</sup> and a broad susceptibility maximum<sup>5</sup> typical of intermediate valence. The compounds are isostructural (with cubic  $\text{AuCu}_3$  structure) and completely miscible<sup>7,8</sup>; hence, the valence instability and the different regimes of magnetic behavior can be obtained by merely alloying. Some other advantages offered by this alloy system are: (i) While alloying introduces disorder, the disorder is primarily on the In-Sn sites; the cerium lattice remains unaltered. Furthermore the In-Sn valence electrons are in  $5s$  and  $5p$  orbitals which may be sufficiently extended that the electron background seen by the cerium electrons might be relatively uniform. (ii) The electronic properties of  $\text{LaIn}_{3-x}\text{Sn}_x$  have been widely studied.<sup>9,10</sup> This isostructural ( $\text{AuCu}_3$ ) system can be used to estimate the non- $4f$  background contributions to the observed behavior.

The magnetic susceptibility of many valence-fluctuation materials shows Curie-Weiss-like behavior at high temperatures  $\chi = C_{\text{eff}}/(T + \Theta)$ , exhibits a broad maximum centered at some temperature  $T_{\text{max}}$ , and is constant at low temperatures,  $\chi(T) \sim \chi(0)$ . This has been discussed in terms of the concept of characteristic-energy behavior.<sup>7</sup> This notion forms the basis of popular experimental phenomenology<sup>11,12</sup>

of mixed valence and is supported by recent inelastic neutron scattering experiments.<sup>13,14</sup> The phenomenology typically invokes two energy scales to explain the susceptibility: a spin-fluctuation frequency  $\hbar\omega_{sf}$  determines the Curie-Weiss parameter  $k\Theta \sim \hbar\omega_{sf}$  while  $C_{eff}$  and  $kT_{max}$  are related to the energy required to promote a nonmagnetic electron into the magnetic orbital. Contrary to this two-energy-scale picture recent results on Yb-based valence fluctuation intermetallics suggest that  $1/\chi(0)$  and  $\Theta$  scale with  $T_{max}$ ,<sup>15,16</sup> as though, within a certain class of compounds, only one energy scale determines  $\chi(T)$ .

Characteristic-energy behavior is theoretically well grounded in dilute magnetic alloys,<sup>17</sup> but this is not the case for nondilute mixed valence. Nevertheless in systems such as<sup>13</sup>  $CePd_3$  and<sup>14,18</sup>  $Ce_{1-x}Th_x$  where both dc susceptibility and inelastic neutron scattering experiments have been performed, characteristic-energy behavior is clearly evident. In particular the frequency-dependent susceptibility is Lorentzian

$$\text{Im}\chi(\omega) \propto \chi_{dc}\omega\Gamma/(\Gamma^2 + \omega^2)$$

We can identify  $\hbar\Gamma$  as a characteristic energy for spin fluctuations,  $kT_{sf}$ , but the definition is somewhat arbitrary, and for our purposes we merely assert that  $\hbar\Gamma = m_1 kT_{sf}$  where  $m_1$  is a constant of order unity. When the dc susceptibility of these materials is examined it is found that

$$\chi(T) = \begin{cases} m_2 C / (T + m_3 T_{sf}), & T \gg T_{sf} \\ C / m_4 T_{sf}, & T \ll T_{sf} \end{cases}$$

and that the broad susceptibility maximum occurs at a temperature representing the crossover from low-temperature to high-temperature behavior:

$$T_{max} = m_5 T_{sf}$$

Here  $C$  is the Curie constant for the free magnetic ion, which for  $J = \frac{5}{2}$  cerium ions is  $C = 0.807$  emu K/mole, and the  $m_i$  are all constants of order unity. Stated in this fashion, the phenomenology accurately describes experiment without being explicitly tied to any assumption about whether one or two energy scales determine  $\chi(T)$ .

The results for the magnetic susceptibility  $\chi(x; T)$  of  $CeIn_{3-x}Sn_x$  presented below will be analyzed in terms of this concept of characteristic-energy behavior. The outstanding feature of the results is that over a broad region of the  $x$ - $T$  diagram, including both trivalent and nonintegral-valent materials, single-energy-scale behavior appears to be valid. In particular the "effective moment"

$$\mu^2(x; T) = T\chi(x; T)/C$$

is found to be a function of a single-scale variable

$$\mu^2(x; T) = \mu^2(T/T_{sf}(x))$$

Alternatively, this means that the constants  $m_i$  are fixed, independent of  $T_{sf}$ ,  $x$ , etc.

Certain other features are worth noting. As was shown in an earlier Letter,<sup>7</sup> the characteristic energy oscillates with  $x$  and is roughly proportional to the conduction-electron density of states. The implication of this for the role of the conduction electrons in controlling the spin fluctuations will be discussed below. Furthermore, within experimental error the high-temperature effective Curie constant is just the free-ion value. Finally the fashion in which the scaling behavior breaks down in indium-rich alloys is revealing: For  $x < 0.4$  there is a low-temperature phase transition into some kind of antiferromagnetic state. In the vicinity of this ordered phase the effective moment is enhanced, as though the magnetic interactions stabilize the moment. The phase diagram for these transitions, which is presented below, is of some interest in its own right, as it may represent an experimental realization of a recently proposed type of phase transition<sup>19</sup>—a  $T = 0$  phase transition from an antiferromagnetic ground state to a nonmagnetic ground state with increasing coupling of the  $4f$  spins to the conduction electrons.

The scaling behavior, newly reported here, was observed only after careful recalibration of the susceptibility measurement, and the results reported here differ in minor ways from the results reported in an earlier Letter.<sup>7</sup> For these reasons, sufficient detail concerning the experimental technique is reported to allow the reader to judge for himself the adequacy of the present procedure and to establish confidence limits on the scaling behavior.

## II. EXPERIMENTAL TECHNIQUE

### A. Sample preparation and analysis

Samples were prepared by melting together the starting materials in an argon arc furnace. The starting materials used, source of supply and their major impurities were: Cerium: United Mineral and Chemical Batch BM338 (20 ppm Al, 30 ppm Ga, 3 ppm Cu, 20 ppm Fe, 10 ppm Mn; interstitial impurities were not listed but were presumably abundant, as in most commercially available rare earths.) Indium: Materials Research Corporation, Marz Grade (10 ppm C, 8 ppm O, 0.6 ppm Fe, 1.0 ppm Si, all others less than 1 ppm). Tin: Alfa Ventron Stock 348. (Listed as better than 99.999% pure with respect to common metals.) Weight losses due to indium evaporation were typically 10 mg in 2 gram samples; the stoichiometry is correspondingly uncertain. The tin-rich samples degrade badly in air; all samples were stored under 100-mTorr vacuum in a dessicator. Despite all such precautions, the major impurities were clearly interstitials (O and H).

A series of seven samples at different concentrations  $x$  were examined under a scanning electron microscope with a fluorescence attachment using magnifications of  $(1-20) \times 10^3$  at the University of Southern California, both to examine the surfaces and estimate stoichiometry. Low-angle powder x-ray diffraction was performed, using the U.C. Riverside GE XRD5 diffractometer, to look for second phases. Further information concerning sample quality was obtained from  $K\alpha$  splittings and linewidths in the high-angle region and from the susceptibility studies themselves.

### B. Determination of lattice constants

Initial lattice-constant studies,<sup>7</sup> carried out at U. C. Riverside, employing the (311) reflection ( $2\theta \sim 65^\circ$ ) are in error; for, as we later learned, the calibration of the instrument changed somewhat with time. The results reported in Fig. 1 were obtained at U. C. Irvine using a Philips back reflection camera (Type 52058) in the parafocusing geometry,<sup>20</sup> which is canonical for lattice-constant determination. The (531) and (600) lines ( $2\theta \sim 160^\circ$ ) were used. This particular camera employs built in calibration marks which minimize radius and film shrinkage corrections and which are static with time. The calibration was checked by measuring the lattice constant of NaCl; the value obtained (5.640 Å) agrees well with values reported in the literature,<sup>21</sup> and was quite stable with time. Values obtained for CePd<sub>3</sub> (4.129 Å), CeIn<sub>3</sub> (4.689 Å) and CeSn<sub>3</sub> (4.722 Å), also agree well with values in the literature.<sup>3,4</sup> We are thus confident that the values of lattice constant reported below are accurate and the ones reported earlier in error. Further-

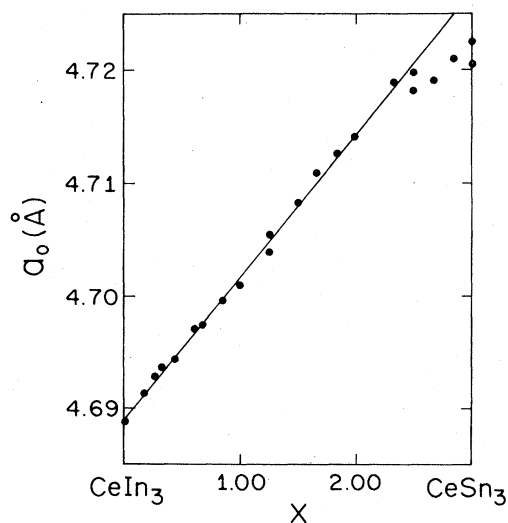


FIG. 1. Room-temperature lattice constants in CeIn<sub>3-x</sub>Sn<sub>x</sub>. The solid line represents Vegard's law.

more the associated error ( $\pm 0.002 \text{ \AA}$ ) is fairly evident from the scatter in the data. This error arises from several sources: the high fluorescence of the rare earths fogs the film, making line centers hard to locate precisely. Further, the samples—particularly the tin-rich alloys—oxidize badly with time, which also obscures the films. Finally, intermediate-valence alloys are sensitive to the sort of strains generated by the powdering process. We hope to correct for these problems in the future by selective filtering and annealing.

### C. Magnetic susceptibility

The magnetic susceptibility was measured using the Faraday technique. Our apparatus includes a Cahn 1000 electrobalance and an Alpha electromagnet with 4 inch constant-force pole pieces. A magnetic field of approximately 3 kG was used. The sample holder, sufficiently heavy to hold the hangdown wire under tension, contributed about 1% of the total signal; this was measured and subtracted out. The apparatus allows translations relative to the magnetic field in all three directions, enabling us to locate the saddle point of  $H dH/dx$  to within 0.3 mm. The effect of thermal expansion of the hangdown wire was measured and found negligible. When the magnetic force exceeded 20 mg, the field was reduced; this helped minimize the effects of lateral instability. The most significant error in our data was induced by the thermometry: a copper-wire thermometer and carbon-glass thermometer were located on the walls of the hangdown tube, thermal contact being made through 1 mm of helium exchange gas. In a separate experiment we measured the temperature at the position of the sample versus the temperature of the walls and found that by keeping the drift rates at less than 10 K per hour the induced error (temperature of the walls minus the temperature of the sample) was a smooth function of temperature, and of a magnitude 1% or less for all temperatures studied.

Absolute calibration of the susceptibility was obtained by measurement of known standards, which were Marz grade metals from Materials Research Corporation. These materials, and their most significant impurities, were Pd (12 ppm Fe), Pt (15 ppm Fe), and Nb (3 ppm Fe, 1 ppm Ni, 200 ppm Ta). The susceptibilities of Pd and Pt are sensitive to these levels of iron impurities.<sup>22</sup> The assay for our Nb sample is quite comparable to sample MRC-2 studied by Collings and Smith<sup>23</sup>; therefore we have adopted their value [ $\chi(300 \text{ K}) = 214.1 \times 10^{-6} \text{ emu/mole}$ ] as our standard. To calibrate successfully requires either that the sample be as small as the volume over which  $H dH/dx$  is constant, or that it be of identical geometry to the calibration standard and located precisely at the same location in the field. We have

adopted the latter method and as a final step in our experiment we very carefully shaped all samples to identical geometry ( $0.393 \pm 0.002$  inches long,  $0.125 \pm 0.002$  inches in diameter) and recalibrated. Following this procedure we obtained the values  $(5.135 \pm 0.025) \times 10^{-6}$  emu/gram for our Pd sample and  $(0.983 \pm 0.005) \times 10^{-6}$  emu/gram for our Pt sample; these values compare quite favorably to the values reported in the literature for Pd and Pt of comparable purity.<sup>22</sup> The effect of the correction was less than a few percent for all samples except  $\text{CeSn}_3$ , which had been investigated earliest in an anomalous geometry. Prior to the shape correction for  $\text{CeSn}_3$  we observed the value  $\chi(300) = 2137 \times 10^{-6}$  emu/mole; after the shape correction we now observe  $\chi(300) = 1840 \times 10^{-6}$  emu/mole in much better agreement with the value  $1880 \times 10^{-6}$  emu/mole reported in the literature.<sup>5</sup> We claim, then, that our calibration procedure is good to about 2% overall. The relative error between samples is better than 0.5% and between temperatures better than 0.1%.

A conservative estimate of the combined error from all sources is 5%; but this includes systematic error, identical in all samples. We are thus confident that the scaling results reported below are good "to a few percent."

### III. RESULTS AND ANALYSIS

#### A. Sample quality analysis

Scanning-electron-microscopy (SEM) results showed that the samples were basically homogeneous, with minor ( $\sim 1\%$ ) inclusions of In-Sn along polishing scratches in the surface and minor ( $\sim 2\%$ ) variations of stoichiometry. Low-angle x-ray diffraction results confirmed<sup>8</sup> that the materials are miscible in all proportions; the  $\text{AuCu}_3$  structure was observed for all alloys. In the high-angle ( $2\theta \approx 160^\circ$ ) scattering the  $K\alpha$  doublets were very well resolved, confirming the basic homogeneity of the alloys.

Surface segregation of tin occurs in  $\text{CeSn}_3$ , which increases with time. Evidence that this is primarily a surface phenomena comes from the fact that freshly powdered samples of  $\text{CeSn}_3$  showed no trace of tin lines in low-angle x-ray spectra—such lines appeared only over the course of time. The process is inhibited by minor indium doping—powder samples with  $x = 1.67$  and  $2.52$  showed no trace of tin or indium lines at the end of a month. We think the effect may be connected with the high reactivity of  $\text{CeSn}_3$  in air; Ce atoms reacting with oxygen or OH groups leave behind free tin which migrates to the surface.

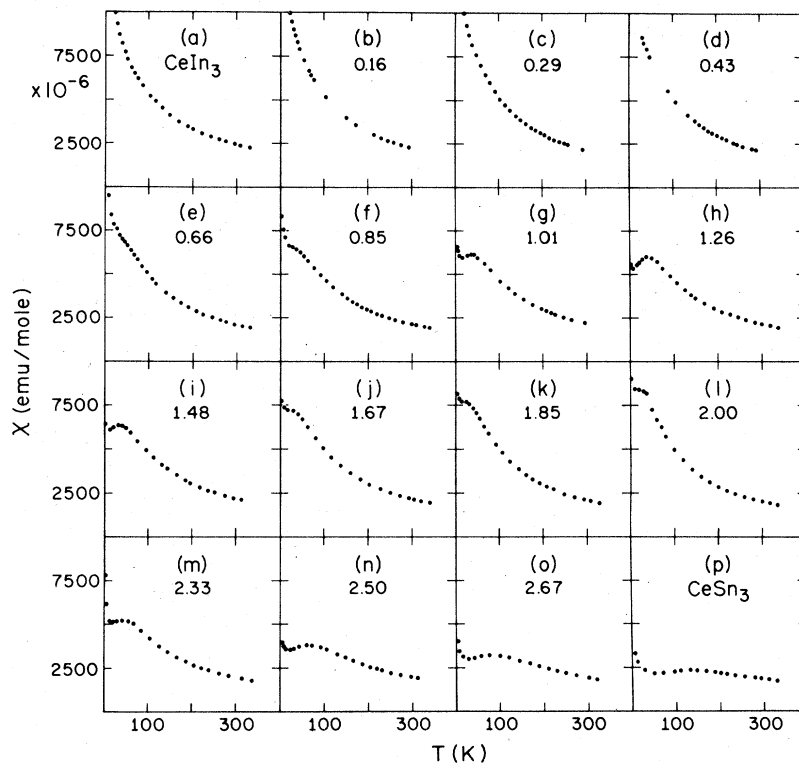


FIG. 2. Susceptibility vs temperature for 16 alloys  $\text{CeIn}_{3-x}\text{Sn}_x$ . The concentrations  $x$  are given in the drawing.

The small ( $< 1 \mu\text{m}$ ) In-Sn inclusions visible in electron micrographs could also be detected in the susceptibility measurement: imposed on the main susceptibility curve was a tiny superconducting transition occurring near 3.5 K, confirmed by measurement of  $M(H)$  at 2.0 K. This effect was only observed for  $0.8 < x < 2.7$  and the superconductivity was type II, as befits  $1\text{-}\mu\text{m}$  particles of In-Sn alloy.

A feature of the low-temperature susceptibility (Fig. 2) is that for  $x \geq 0.8$  there is a Curie contribution. For  $2 < T < 20$  K the susceptibility can be fit to better than  $\frac{1}{2}\%$  in the form

$$\chi(T) = \chi(0) + nC/T,$$

where  $C$  is the  $J = \frac{5}{2}$  free-ion Curie constant and  $n$  is typically 0.003. Such an effect can have several origins: it can arise from magnetic impurities in the sample, or from cerium atoms which are stabilized in the trivalent state due to local strain fields or oxidation. The effect does not reproduce for different samples made from identical starting materials. It would be straightforward to subtract this contribution from the data, but we prefer to let it remain, for two reasons: first, it has only a minor effect on any of the results reported below; and second, at least for  $0.6 < x < 1.5$ , the effect may be in part intrinsic, arising from a local environment effect where cerium atoms completely surrounded by indium atoms remain trivalent to very low temperatures.

We performed annealing studies on several samples, annealing at  $900^\circ\text{C}$  for two days. Following the anneal we observed enormous increases in the "impurity" contribution (to values of  $n$  as large as 0.1). For this reason we decided to study the samples in the as-melted condition.

### B. Lattice-constant results

The lattice constants  $a_0(x)$ , observed at room temperature, are plotted in Fig. 1. The striking feature is that while Vegard's law is obeyed for  $0 < x < 2.3$ , significant deviations, outside the limits of error ( $\pm 0.002 \text{ \AA}$ ), occur for the tin-rich alloys.

### C. Susceptibility results

The susceptibility for 16 alloys is plotted in Fig. 2. Reproducibility runs were performed on alternate samples for eight values of  $x$ , with identical results. The significant aspect of the data is that while all samples exhibit Curie-Weiss-like behavior at high temperatures, those samples with  $x \geq 0.8$  exhibit broad susceptibility maxima and constant low-temperature susceptibility whereas samples with  $x \leq 0.6$  are monotone increasing with decreasing  $T$

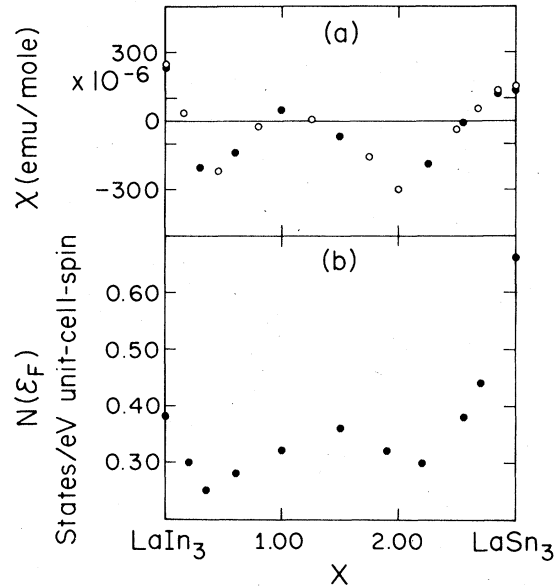


FIG. 3. (a) Room-temperature susceptibility of  $\text{LaIn}_{3-x}\text{Sn}_x$ . Solid circles are the data of Ref. 9; open circles are our data. This susceptibility is interpreted as the non- $4f$  background of  $\text{CeIn}_{3-x}\text{Sn}_x$ , and is subtracted from the data of Figs. 4 and 5. (b) Density of states at the Fermi surface  $N(\epsilon_F; x)$  in  $\text{LaIn}_{3-x}\text{Sn}_x$ , deduced from linear coefficients of specific heat in Ref. 10. This is interpreted as representing the conduction-band density of states, prior to hybridization with the  $4f$  electron, in  $\text{CeIn}_{3-x}\text{Sn}_x$ .

down to either the lowest temperature measured or to the temperature of the phase transitions reported below.

The susceptibility of  $\text{CeIn}_{3-x}\text{Sn}_x$  arises mainly from the  $4f$  electrons, but contributions are expected from the other electrons; and in particular the lanthanide  $5d$  electrons make a significant contribution. An estimate of this effect can be obtained from Fig. 3 where we plot the susceptibility of  $\text{LaIn}_{3-x}\text{Sn}_x$ . The contribution is as much as 10% at room temperature. While this background varies weakly with temperature, the  $4f$  susceptibility of  $\text{CeIn}_{3-x}\text{Sn}_x$  in all but the most tin-rich samples is several times larger at low temperatures than at 300 K. Thus the correction is typically quite small at low temperatures and its temperature variation can be safely ignored in all samples except  $\text{CeSn}_3$ . Thus we define the  $4f$  susceptibility of  $\text{CeIn}_{3-x}\text{Sn}_x$  as

$$\chi_{4f}(x, T) = \chi(x, T) - \chi_{\text{La}}(x, 293),$$

where  $\chi_{\text{La}}(x, T)$  is the susceptibility of  $\text{LaIn}_{3-x}\text{Sn}_x$  at the same concentration  $x$ .

The inverse of this  $4f$  susceptibility is plotted in Fig. 4. The Curie-Weiss behavior is apparent in this figure; the solid lines represent the prediction  $C'(x)/[T + \Theta'(x)]$  where the values of  $C'(x)$  and

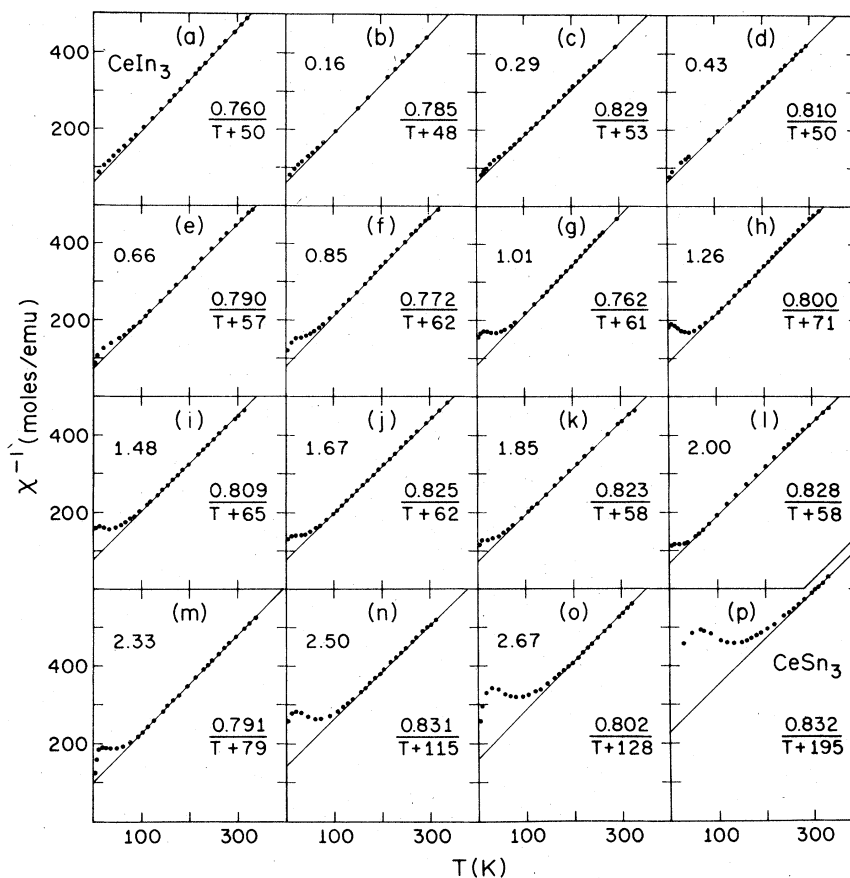


FIG. 4. Inverse 4f susceptibility (corrected for non-4f background) for 16 alloys of  $\text{CeIn}_{3-x}\text{Sn}_x$ . The concentrations  $x$  are given in the drawing, as well as the asymptotic high-temperature Curie-Weiss behavior  $\chi = C(x)/[T + \Theta(x)]$ . The units of  $C(x)$  are emu K/mole.

$\Theta'(x)$  are given for each sample. In Fig. 5 we plot the "effective moment"

$$\mu^2(x; T) = T\chi_{4f}(x; T)/C,$$

where  $C$  is the Curie constant for the free  $J = \frac{5}{2}$  ion, 0.807 emu K/mole. The plot has a logarithmic abscissa; such a semilog plot is convenient for testing for scaling<sup>17(b)</sup>: if  $\mu^2(x, T)$  is a function of a scaled variable  $\mu^2(x, T) = \mu^2(T/T_{sf}(x))$  then all curves can be made to coincide by a horizontal shift so that the  $T_{sf}(x)$  match up. The solid lines in the figure represent a smooth curve drawn through the data for the sample  $x = 1.85$ ; this curve was then shifted horizontally to fit the data for the other samples. [Note that it is irrelevant for this purpose which temperature on the "universal" curve actually represents  $T_{sf}$ . As a reasonable estimate we choose the temperature  $T^*$  at which  $\mu^2$  falls to the value 0.5; the values of  $T^*(x)$  are included in the drawing.] The outstanding feature is that for  $x \geq 0.8$  all samples follow the same curve, as a function of  $T/T_{sf}$ , to within a few per-

cent, even though  $T_{sf}$  varies by a factor of 4.

Uncertainty in estimating the asymptotic high-temperature regime and the sensitivity of Curie-Weiss fits to thermal lag effects (notable as a small glitch in the vicinity of 293 K) make the uncertainty in the value of  $C'(x)$  and  $\Theta'(x)$  be of order 5%. On the other hand the "effective moment" plots make no assumptions about the behavior of the susceptibility; the value of  $C$  used is that of the free ion, which can be calculated. Furthermore the logarithmic temperature scale puts thermal lag error (which is typically 1% or less) on an equal footing for all temperatures. A potential objection is that the magnitude of the low-temperature moment is *not* treated on an equal footing with the high-temperature moment. However, the behavior below 20 K is uncertain due to the above mentioned impurity contribution, which contributes an additive constant  $n \sim 0.003$  to  $\mu^2$ . This is quite small on our absolute scale, but significant on a relative scale. We prefer to ignore variations in  $\mu^2$  at low temperatures which do not stand out clearly on the absolute scale, and argue that this method of data

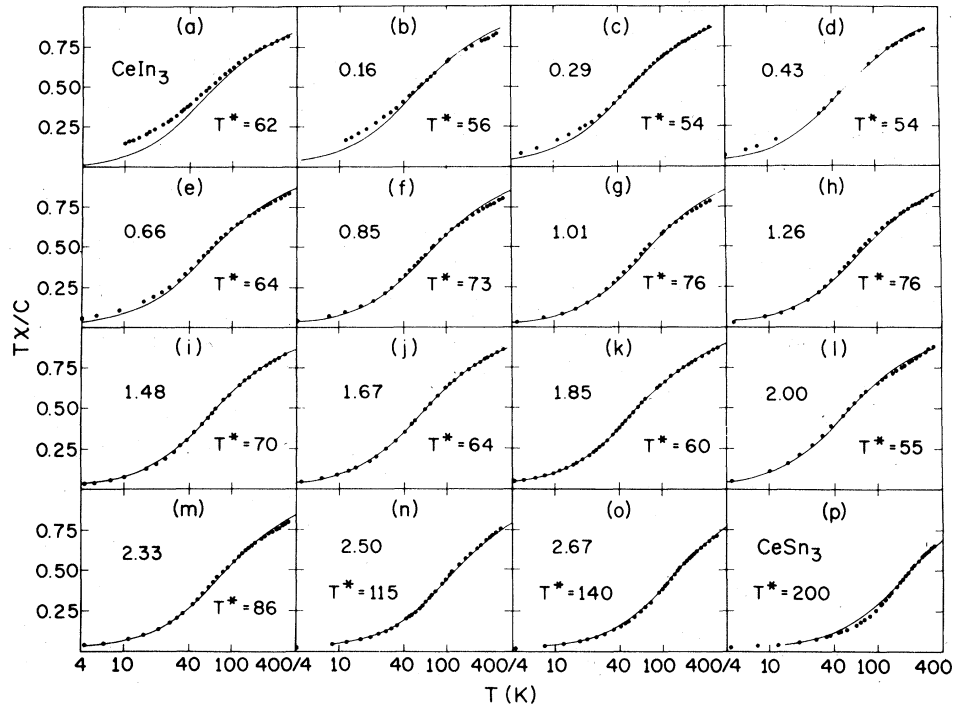


FIG. 5. Effective moment  $\mu^2 = TX/C$  for 16 alloys of  $\text{CeIn}_{3-x}\text{Sn}_x$ .  $C = 0.807$  emu K/mole is the free-ion Curie constant. The concentrations, and the temperatures  $T^*$  at which  $\mu^2(T^*) = \frac{1}{2}$  are given in the figure. The solid line represents a solid line drawn through the data of one sample ( $x = 1.85$ ), shifted horizontally to match all other samples. On such a semilogarithmic plot this demonstrates that the effective moment is a function  $\mu^2(T/T_{sf})$  of a scaled variable. Note that this scaling occurs for  $0.8 < x < 3.0$ , but breaks down strongly in the indium-rich samples.

analysis is really quite appropriate for mixed-valence materials, where the key feature is a vanishing moment.

The degree to which  $\mu^2(T, x)$  follows the same curve, as a function of scaled variable for all  $x$ , depends somewhat on subtraction of the non- $4f$  background susceptibility. It is reasonable to argue that the non- $4f$  background in  $\text{CeIn}_{3-x}\text{Sn}_x$  may be substantially different from the susceptibility of  $\text{LaIn}_{3-x}\text{Sn}_x$ . There is, however, a very interesting self-consistency check on this procedure. In Fig. 6 we plot the Curie constants  $C(x)$ , obtained from data similar to that of Fig. 4 but prior to the subtraction procedure, and  $C'(x)$ , the Curie constants obtained from Fig. 4 after the subtraction. The dashed line represents the value  $C = 0.807$  emu K/mole calculated for free  $J = \frac{5}{2}$  spins. Prior to the subtraction there is a marked oscillation in the Curie constant; and in  $\text{CeIn}_3$  ( $\text{CeSn}_3$ ) the Curie constant is enhanced by 12 (20) percent over the free-ion value—a rather strange result in a system where the coupling of  $4f$  spins to conduction electrons is expected to be antiferromagnetic. However, it can be seen that the oscillation in  $C(x)$  tracks the oscillation in  $\chi_{\text{La}}(x; 293)$  (see Fig. 3), and when the latter is subtracted out the

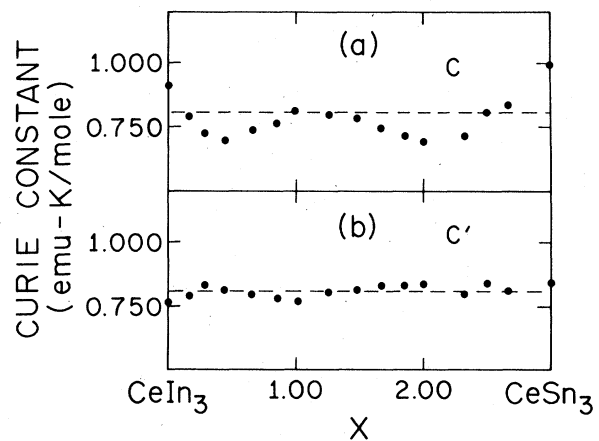


FIG. 6. (a) Curie constants of  $\text{CeIn}_{3-x}\text{Sn}_x$  deduced from plots similar to Fig. 4, but prior to subtraction of the non- $4f$  contribution, Fig. 3. (b) Curie constants as deduced from Fig. 4, after subtraction of the background. The dashed line in (a) and (b) represents the  $J = \frac{5}{2}$  free-ion value  $C = 0.807$  emu K/mole. Apparently the oscillation observed in (a) arises from the oscillation in the non- $4f$  background; when subtracted, all  $C'(x)$  become equal to the free-ion value within experimental error.

resulting  $C'(x)$ , to within experimental error, takes on the free-ion value for all  $x$ . This, it seems to me, is more plausible physically than the large oscillation, and supports the subtraction procedure.

In Fig. 7(a) we plot the Weiss parameters  $\Theta(x)$ , obtained before the background  $d$ -orbital subtraction; and in Fig. 7(b) the values  $\Theta'(x)$  after the subtraction. In addition we plot the values  $T^*(x)$  at which  $\mu^2(x, T) = \frac{1}{2}$ , taken from Fig. 5. It is of interest to note that  $T^*(x) \approx \Theta'(x)$ . If we arbitrarily choose  $T_{sf} = T^*$  this implies that the high-temperature behavior is

$$\chi(T) = C/(T + T_{sf})$$

where  $C$  is the free-ion value, i.e., in terms of our earlier discussion,  $m_2 = m_3 = 1$ . In Fig. 8 we plot  $T_{max}(x)$ , the temperatures of the susceptibility maxima, as well as the inverse  $T=0$  susceptibility  $C/\chi(0)$  where  $\chi(0)$  is extracted from the low-temperature

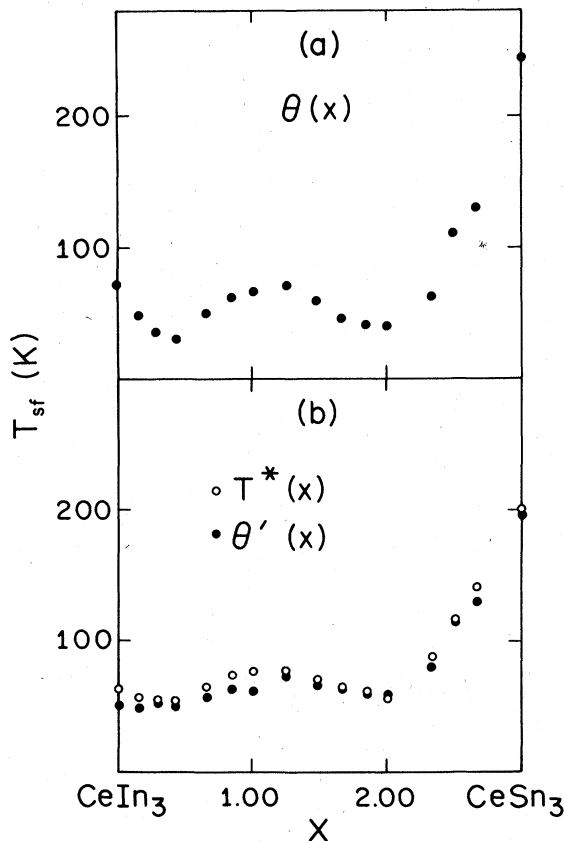


FIG. 7. (a) Values of the Weiss parameters of  $\text{CeIn}_{3-x}\text{Sn}_x$  deduced from data similar to Fig. 4 but prior to subtraction of the non- $4f$  background. (b) Values of the Weiss parameters  $\Theta'$  deduced from Fig. 4, after background subtraction, and values of  $T^*$  deduced from Fig. 5. Note the near equality of  $T^*(x)$  and  $\Theta'(x)$ .

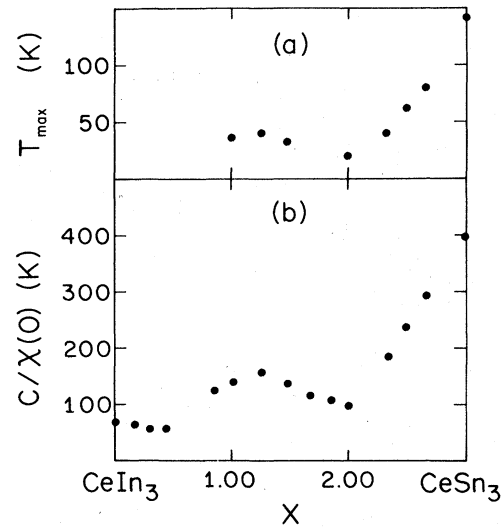


FIG. 8. (a) Temperatures  $T_{max}(x)$  where the susceptibility maxima occur in  $\text{CeIn}_{3-x}\text{Sn}_x$ . (b) Inverse low-temperature susceptibility  $C/\chi(x; T=0)$ , estimated as indicated in the text.

behavior using  $\chi(T) = \chi(0) + nC/T$  as discussed above. [For  $x < 0.6$  the largest observed value of  $\chi$ —either  $\chi(2 \text{ K})$  or  $\chi(T_N)$ —was used to estimate  $\chi(0)$ ]. From these data we conclude  $m_4 \approx 2$  and  $m_5 \approx \frac{1}{2}$  for the choice  $T_{sf} = T^*$ . (Regardless of the choice of  $T_{sf}$ , we conclude that  $m_5:m_4:m_3 = 1:4:2$ .)

The subtraction of the nonmagnetic background has the effect of reducing the amplitude of the oscillations observed in  $\Theta(x)$  (Fig. 7). For the reasons given above, however, we argue that there is less error involved in determining  $T^*$  than in determining  $\Theta$ . Since the oscillation in  $T^*$ ,  $T_{max}$ , and  $C/\chi(0)$  are quite marked and since all three are proportional to  $T_{sf}$ , we assert that  $T_{sf}(x)$  exhibits a pronounced oscillation with  $x$ , as reported in the earlier Letter<sup>7</sup> and discussed further below.

In Fig. 9 we exhibit the low-temperature phase transitions which occur in the indium-rich samples. Without direct knowledge of the microscopic spin structure from neutron scattering, we can only assert that the ordering must be some version of antiferromagnetism. On general grounds one expects a divergence in the slope  $d\chi/dT \sim A|T - T_N|^{-\alpha}$  to occur at  $T_N$ , which can imply that  $T_N$  occurs at either a cusp or an inflection point of  $\chi$ , depending on the value of  $\alpha$  and  $A$ . The maximum at 10.1 K in  $\text{CeIn}_3$  is sufficiently sharp that it is impossible to determine whether the singularity is located at the maximum or in very close proximity. (The source of the difficulty resides in our thermometry, where thermal contact between thermometer and sample, through helium exchange gas, is insufficiently intimate for a real critical-point study.) The phase transitions for larger



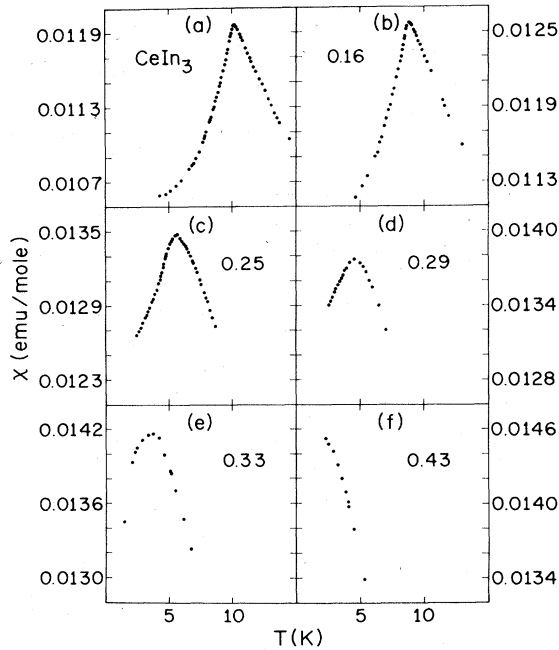


FIG. 9. Susceptibility near the phase transitions in indium-rich samples of  $\text{CeIn}_{3-x}\text{Sn}_x$ . The concentrations  $x$  are given in the drawing. The maxima suggest the spin ordering is some sort of antiferromagnetism.

$x$  exhibit increasingly broadened maxima—the broadening undoubtedly reflects inhomogeneity rounding, which has a particularly pronounced effect for those values of  $x$  where the phase boundary is steep [i.e., where  $T_N(x)$  varies rapidly with  $x$ ]. Choosing  $T_N(x)$  as the temperature of the maxima,

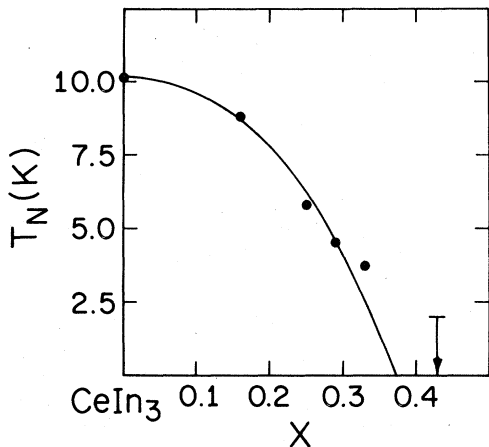


FIG. 10. Phase diagram for the magnetic phase transitions deduced from Fig. 9, identifying  $T_N(x)$  as the temperature of the susceptibility maxima. There is a  $T=0$  phase transition at  $n_c \approx 0.4$  from the magnetic ground state to a trivalent, nonordered, spin-fluctuation ground state.

we plot the phase boundary  $T_N$  vs  $x$  in Fig. 10. There is clearly a critical concentration  $n_c \sim 0.4$  where  $T_N \rightarrow 0$ . Given the reservations concerning choice of  $T_N$  for those samples with inhomogeneity broadening, it is impossible to locate  $n_c$  very precisely, nor to tell whether  $dT_N/dx$  is finite or infinite as  $n \rightarrow n_c$ . Nevertheless the main feature of the phase diagram is evident: there is a  $T=0$  phase transition with increasing  $x$  from an ordered state, where the ordering is some kind of antiferromagnetism, to a nonmagnetic ground state; the critical concentration is of order 0.4.

#### IV. DISCUSSION

##### A. Valence instability and the lattice constant

In the study of valence fluctuation materials it has become traditional to estimate the  $4f$  occupation number (i.e., the valence itself) from lattice-constant extrapolations, the assumption being made that the valence and lattice constant are linearly related. While it would seem desirable to determine the valence more directly—e.g., from integrated intensities in an x-ray photoemission spectroscopy (XPS) experiment—in fact, all such methods themselves assume some form of linear relationship to the valence, which can be questioned. Without a well established theory of mixed valence, all techniques are equally suspect. Furthermore, the sensitivity available in a lattice-constant measurement is as good or better than most competing methods. Hence, we argue, determination of valence from anomalous lattice constants is at present very reasonable.

In this spirit we examine the lattice-constant results for  $\text{CeIn}_{3-x}\text{Sn}_x$ , presented in Fig. 1. In older investigations<sup>4</sup> of these intermetallics the conclusion was drawn that  $\text{CeIn}_3$  is trivalent while the valence of  $\text{CeSn}_3$  at 293 K is greater than 3.1. Since Vegard's law is well satisfied for  $0 < x < 2.3$ , the simplest interpretation of Fig. 1 is that the metals are trivalent for  $0 < x < 2.3$  and that nonintegral valence sets in continuously for larger  $x$ .

The valence of these materials is never far from three, however, and alternative assignments of the valence are possible. For example, the valence may vary smoothly from three to a nonintegral value for  $x = 2.3$ , varying more rapidly for larger  $x$ ; or, keeping in mind the reservations about the linearity between  $a_0$  and the valence, it is plausible that  $\text{CeSn}_3$  is itself trivalent. Nonetheless, the deviation from Vegard's law is unmistakable, as is the deviation of  $a_0$  in  $\text{CeSn}_3$  from its expected trivalent value.<sup>4</sup> We thus feel that the simple interpretation—that there is a valence instability with increasing  $x$  from trivalence for  $x < 2.3$  to nonintegral valence for larger  $x$ —should be given considerable weight.

### B. Characteristic-energy (scaling) behavior

The results presented above clearly indicate that single-energy-scale characteristic-energy behavior is valid in  $\text{CeIn}_{3-x}\text{Sn}_x$ , over a wide interval of characteristic energies ( $55 \text{ K} < T^* < 200$ ). To recapitulate, the main features are that the effective moment  $\mu^2(x; T) = T\chi(x, T)/C$  is a universal function of  $T/T_{\text{sf}}(x)$ ; and if we (arbitrarily) define  $T_{\text{sf}} = T^*$  [defined implicitly by  $\mu^2(T^*) = \frac{1}{2}$ ] the susceptibility obeys

$$\chi \approx \begin{cases} C/(T + T_{\text{sf}}) & , T \gg T_{\text{sf}} \\ C/2T_{\text{sf}} & , T \ll T_{\text{sf}} \end{cases}$$

and has a broad maximum at  $T_{\text{max}} \approx \frac{1}{2} T_{\text{sf}}$ .

Without testing this in a broader class of materials, i.e., without knowledge of its general validity, of whether it is merely a fortuitous property of one isolated alloy system, it is dangerous to be overly assertive about the significance of this result. However, there *are* indications in the literature<sup>15,16</sup> that such scaling behavior is more generally valid, so it is worthwhile to spend some time discussing its potential significance.

First of all, it seems that there is no direct correlation between the magnetic properties and the valence. The magnetic behavior falls into two categories: For small  $x$  the susceptibilities are monotone and magnetic ordering occurs; there is no maximum or significant flattening in the vicinity of  $\frac{1}{2} T^*$ . For  $x \geq 0.8$  the susceptibility shows a maximum, and the scaling feature holds; i.e., all susceptibilities are essentially identical. The region  $0.4 < x < 0.8$  corresponds to a crossover between these kinds of behavior. This crossover does *not* correspond, however, to what we believe to be the crossover from trivalence to intermediate valence ( $x \sim 2.3$ ). This fact might appear to suggest that the magnetic behavior in the trivalent spin-fluctuation regime is identical with that in the intermediate-valence regime. However,  $\text{CeSn}_3$  exhibits only weak mixed-valence character and it is plausible that the scaling behavior is just beginning to break down near  $x = 3.0$ . It is really an open question whether the single-energy-scale characteristic-energy behavior is valid for strong intermediate valence.

It is useful to consider the results of calculations for the asymmetric Anderson model<sup>17,24</sup> as a guide for further discussion of our results. In that theory scaling behavior is observed when the  $4f$  level is sufficiently far below the Fermi surface, i.e., when Kondo theory is applicable; the moment scales with the Kondo temperature,  $T_K$  and  $\mu^2 = \mu^2(T/T_K)$ . The basic physics is that a zero-order spin demagnetizes due to virtual transitions from  $4f$  level to the Fermi surface. At high temperatures  $\chi \approx 0.7C/(T + 2T_K)$ .

When the  $4f$  level is sufficiently far above the Fermi level the basic picture is a zero-order singlet with modifications due to Van Vleck like virtual transitions from the Fermi surface into the  $4f$  orbital. The effective moment builds up rapidly in the vicinity of  $kT = \Delta\epsilon = E_f - \epsilon_f$ ; the curve is steeper than that curve which is universal in the Kondo regime. Energies  $\Delta\epsilon \approx 0$  represent a crossover between these two kinds of behavior; not too surprisingly the universality breaks down and two energy scales [essentially  $\Delta\epsilon$  and the hybridization width  $N(\epsilon_f)V_{kf}^2$ ] determine  $\mu^2$ . Indeed, the two-energy-scale phenomenology<sup>11</sup> quite accurately describes the main features of the susceptibility of the single-impurity model when  $\Delta\epsilon \approx 0$ .<sup>17(a)</sup>

While we do not intend to imply that the single-impurity theory adequately describes concentrated mixed-valence materials, nevertheless it is plausible that a similar sequence of behavior should occur in the intermetallics. The trivalent spin-fluctuation regime ( $E_f < \epsilon_f$ ) is the analogue of the Kondo regime, and it is here that the scaling is observed. Intermediate valence represents a crossover towards tetra-valence, and we might well expect the scaling behavior to break down if we could probe into the strongly intermediate-valence region. Hence the relevance of the two-energy-scale phenomenology remains open, as it may not be applicable for strong intermediate valence. Another feature of the single-impurity model calculation which is expected on qualitative grounds is a reduction of the Curie constant when  $kT$  becomes much greater than  $\Delta\epsilon$ ; this arises because the ion then has finite probability of being in the nonmagnetic state. The two-scale phenomenology predicts a Curie constant for cerium of  $(\frac{6}{7})C$ . Although this is well outside the bounds of error of the Curie constants actually observed, it is plausible that there could be such a reduction of effective moment at sufficiently high temperature.

Several other questions need to be addressed. One concerns the role of crystal fields in the demagnetization. In cubic symmetries the  $J = \frac{5}{2}$  moment splits into a doublet (lowest) and a quartet<sup>25</sup>; the typical splittings in cerium intermetallics are  $\Delta \approx 50 \text{ K}$ . The effective moment for a  $J = \frac{5}{2}$  ion subject to such a crystal field is significantly reduced only at temperatures appreciably smaller than  $\Delta$ .<sup>18</sup> This should have only a minor effect on the  $\mu^2$  curves, at the lowest temperatures.

In an alloy, local environment effects may contribute to the magnetic properties, the idea being that those cerium ions surrounded mostly by indium atoms should be less likely to demagnetize. It is possible that the low-temperature "impurity" susceptibility observed for  $0.6 < x < 1.5$  to some extent represents such an intrinsic effect. For all  $x$  in the interval  $[0.66 \leq x \leq 3.0]$  the susceptibility between

2–18 K can be fit to better than 1% in the form

$$\chi(T) = \chi(0) + nC/T,$$

where  $C$  is the  $J = \frac{5}{2}$  free-ion Curie constant and  $n$  is a small fraction. Suppose for the moment that this low-temperature Curie law arises from those cerium atoms completely surrounded by indium atoms. The probability that a given cerium atom has indium atoms on all 12 nearest-neighbor sites is

$$p(12;x) = [(3-x)/3]^{12}.$$

Thus if the effect is intrinsic we might expect that  $n$  is proportional to  $p(12;x)$ ; i.e.,  $n(x) = Ap(12;x)$ . In Fig. 11 we plot the observed values of  $n(x)$  together with a plot of  $p(12;x)$  where the proportionality constant  $A = 0.46$  is fixed such that  $n(0.66) = Ap(12;x = 0.66)$ . From this plot we see first of all that the low-temperature behavior cannot be entirely intrinsic:  $n(x)$  does not reproduce well for different samples at the same concentration, and it is too large for  $x > 1.50$ . However the results shown in Fig. 11 are suggestive that between 0.6 and 1.5 the effect indeed may be at least in part intrinsic. However, as we

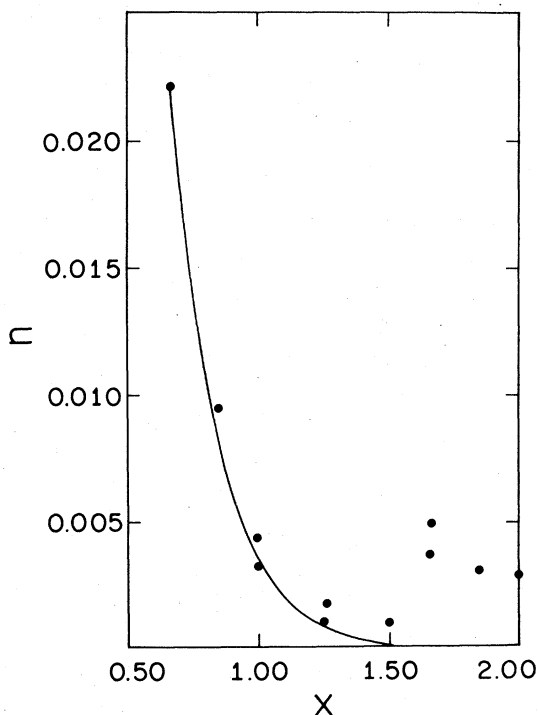


FIG. 11. "Impurity fraction"  $n$  vs  $x$  where  $n(x)$  is extracted from the low-temperature susceptibility  $\chi(T) = \chi(0) + n(C/T)$ . The solid line is proportional to the fraction of cerium atoms surrounded by 12 nearest-neighbor indium atoms (see the text for further explanation).

have already commented, the contribution of the low-temperature feature to  $\mu^2$  is quite small—without ruling out the possibility of local environment effects, we argue that they have only small effect on the scaling results. It is plausible that because the Sn-In valence electrons are in  $5s$  and  $5p$  orbitals, which are presumably fairly extended, the  $4f$  electrons see a conduction-electron background which is sufficiently uniform to reduce local environment effects.

### C. Oscillation in the characteristic energy

In an earlier Letter<sup>7</sup> we discussed the oscillation of  $T_{sf}(x)$ , arguing that it is evidence that  $4f$ -conduction-electron coupling is responsible for the spin-fluctuation behavior. So that the article will be self-contained, we repeat the argument here. The density of states at the Fermi surface,  $N(\epsilon_F; x)$ , for  $\text{LaIn}_{3-x}\text{Sn}_x$  is shown in Fig. 3. We derived this graph utilizing existing data<sup>10</sup> for the linear coefficient of the specific heat, and applying the formula

$$\gamma = \frac{2}{3} \pi^2 k_B^2 N(0).$$

A more sophisticated treatment,<sup>9</sup> where the electron-phonon enhancement  $(1 + \lambda)$  is estimated from existing data, gives essentially similar (though slightly smaller) values for  $N(0)$ . If we adopt the additide that the conduction-electron density of states of  $\text{CeIn}_{3-x}\text{Sn}_x$ , prior to hybridization with the  $4f$  electrons, is given by  $N(\epsilon_F; x)$  for the lanthanum isomorph, then it is clear that the oscillation in  $T_{sf}(x)$  and  $N(\epsilon_F; x)$  are roughly proportional.

Such a proportionality could arise in several ways: the characteristic energy could be simply proportional to the hybridization width

$$kT_{sf}(x) \sim N(\epsilon_F; x) V_{kf}^2.$$

We could then use our results to estimate  $V_{kf}$  which would be of order 0.15 eV. Alternatively if a Kondo-like formula were applicable

$$kT_{sf} \propto \exp[-1/N(0)\mathcal{J}],$$

where  $\mathcal{J}$  is the  $f$ - $s$  coupling constant, it would also follow that  $T_{sf}$  would increase as  $N(0)$  increases. At the least these give us some notion of how the conduction electrons would contribute to the determination of the characteristic energy. In any case the mutual oscillation of  $N(\epsilon_F)$  and  $T_{sf}$  is fairly direct evidence that the conduction electrons are important in the demagnetization.

The origin of the oscillation in  $N(\epsilon_F)$  has been discussed in earlier publications.<sup>9,10</sup> It seems to be a fairly general property in a wide class of similar alloys

in the AuCu<sub>3</sub> structure and hence associated with a rather general feature of the band structure.

Another interesting relevant feature of the older work is that it is argued therein<sup>9</sup> that the oscillation in the density of states tracks the local density of states on the tin-indium sites better than on the lanthanide sites. In order not to violate parity, 4*f* electrons are supposed to hybridize onto neighboring sites.<sup>2</sup> It is thus reasonable that the strength of the hybridization should primarily track the local density of states at the tin-indium site.

#### D. Magnetic-phase diagram

The magnetic-phase transitions that occur in the indium-rich alloys are of considerable interest, as they occur in a region where the magnetic interactions compete with the spin fluctuations which tend to demagnetize the local electrons. A similar situation occurs in CeAl<sub>2</sub>,<sup>1</sup> in which the magnetic ordering has a fairly exotic (primarily antiferromagnetic) configuration.<sup>26</sup> In the absence of microscopic information we can only conclude from the sharp susceptibility maxima of CeIn<sub>3</sub> that the ordering must be some form of antiferromagnetism.

Recent theoretical work<sup>19</sup> in a one-dimensional "Kondo-lattice" model in which the local spins are coupled to the conduction electrons by an antiferromagnetic exchange interaction  $-\mathcal{J}\vec{\sigma} \cdot \vec{S}_f$  predicts a  $T=0$  phase transition from an antiferromagnetic ground state to a nonmagnetic ground state as  $\mathcal{J}$  increases. The relevance of this model [ which is one-dimensional and which ignores the charge (valence) fluctuations on the 4*f* sites ] to real mixed-valence materials is not established. However it is interesting to discuss the magnetic-phase diagram of CeIn<sub>3-x</sub>Sn<sub>x</sub> in this context, since there is a  $T=0$  phase transition from an antiferromagnetic ground state to a trivalent nonmagnetic ground state as  $x$  increases. To complete the analogy we would have to show that  $\mathcal{J}$  increases with  $x$ . One way to determine  $\mathcal{J}$  is to assume that a Kondo-like formula holds for  $0 < x < 0.4$

$$T_{sf}(x) \propto \exp[-1/N(0;x)\mathcal{J}(x)] .$$

$N(0;x)$  can be obtained from Fig. 3; it is seen to decrease by a factor of  $\frac{3}{2}$  as  $x$  increases from 0 and 0.4.  $T_{sf}(x)$  can be obtained from Fig. 7; however since in that figure  $T_{sf}$  represents  $T^*$  or  $\Theta$ , and as both these quantities are influenced by antiferromagnetic interactions, we need to estimate the effect of such interactions on  $\Theta$  and  $T^*$ . The simplest assumption is that

$$\Theta(x) = T_{sf}(x) + T_N(x) .$$

Adopting this, we see that  $T_{sf}(x)$  is constant, or

perhaps even weakly increasing, as  $x$  increases in the interval [0, 0.4]. We might then indeed conclude that  $\mathcal{J}(x)$  increases, by a factor of  $\frac{3}{2}$ , in this interval.

What we *can* say is that if in the trivalent regime  $0 < x < 0.4$  the spin-fluctuation temperature  $T_{sf}$  is determined by a Kondo-like formula, then the  $T=0$  phase transition from an antiferromagnetic to a trivalent nonmagnetic ground state coincides with increasing 4*f*-conduction-electron coupling.

The breakdown of the scaling result in the vicinity of the phase transitions occurs in such a way that the low-temperature effective moment becomes increasingly enhanced over the scaling curve value as  $x \rightarrow 0$ , even for  $T > T_N$ . This occurs simultaneously to the tendency of the antiferromagnetic interactions to reduce the bulk moment. Apparently the interactions stabilize the local moment on an ion faster than they reduce the moment in the bulk. This result can be viewed the other way around: the effect of the increasing importance of spin fluctuations as  $x$  increases is to strongly decrease the magnitude of the low-temperature local moment—this will presumably be true as well in the magnetic ground state, where the  $T=0$  local moment should vanish as  $n \rightarrow n_c$ .

#### V. CONCLUSION

The physics presented by the valence fluctuation system CeIn<sub>3-x</sub>Sn<sub>x</sub> is quite rich: there is a valence transition from trivalence to nonintegral valence, a  $T=0$  phase transition from a magnetic to a nonmagnetic ground state, characteristic-energy behavior occurs in a particularly stringent form, and oscillations in conduction-electron properties are reflected in the characteristic energy for spin fluctuations.

Scaling behavior is a very significant aspect of several important physical problems, e.g., phase transitions or the Kondo effect. The significance of the scaling results in CeIn<sub>3-x</sub>Sn<sub>x</sub> is, however, not clear. The mixed-valence problem is a vastly more difficult problem than the single-impurity problem, with important expected differences.<sup>27</sup> Hence analogies to scaling behavior in the Kondo problem should not be overstressed. But it is straightforward to examine this kind of behavior experimentally, and it is clear that further experiments are in order—to examine the behavior of the effective moment in a broader class of materials, at higher temperatures, and over a broader span of valency. Such experiments are indeed being planned as part of our ongoing program.

Neutron scattering experiments are also underway in this system. Hopefully these will determine the relationship between the macroscopic characteristic-energy behavior and the underlying spin dynamics; in addition the magnetic phase transition will be explored, and the role of crystal fields will be examined.

## ACKNOWLEDGMENTS

This work was supported by the NSF under Grant No. DMR76-82109. Several individuals contributed to portions of this work, most notably David Murphy, but also Greg Beall, Kelly Dunn, Garik Gharibianians and Chuck Sword. Zack Fisk of U.C. San

Diego and Doug MacLaughlin of U. C. Riverside contributed use of their metallurgical facilities. We have benefited from discussions with Professor MacLaughlin, and from the ongoing support and interest of Doug Mills and Peter Riseborough. Chandra Varma kindly read and provided helpful criticisms of an earlier version of this report.

- <sup>1</sup>*Valence Instabilities and Related Narrow-band Phenomena*, edited by R. D. Parks (Plenum, New York, 1977).
- <sup>2</sup>C. M. Varma, *Rev. Mod. Phys.* **48**, 219 (1976).
- <sup>3</sup>I. R. Harris, M. Norman, and W. E. Gardner, *J. Less-Common Met.* **29**, 299 (1972).
- <sup>4</sup>I. R. Harris and G. V. Raynor, *J. Less-Common Met.* **9**, 7 (1965).
- <sup>5</sup>T. Tsuchida and W. E. Wallace, *J. Chem. Phys.* **43**, 3811 (1965).
- <sup>6</sup>H. J. van Daal and K. H. J. Buschow, *Phys. Status Solidi* **3**, 853 (1970).
- <sup>7</sup>J. Lawrence and D. Murphy, *Phys. Rev. Lett.* **40**, 961 (1978).
- <sup>8</sup>L. B. Welsh and J. B. Darby, Jr., in *Proceedings of the 18th Conference on Magnetism and Magnetic Materials, Denver, 1972*, edited by C. D. Graham, Jr. and J. J. Rhyne, AIP Conf. Proc. No. 8 (AIP, New York, 1973), p. 1325.
- <sup>9</sup>A. M. Toxen, R. J. Gambino, and L. B. Welsh, *Phys. Rev. B* **8**, 90 (1973).
- <sup>10</sup>W. D. Grobman, *Phys. Rev. B* **5**, 2924 (1972).
- <sup>11</sup>B. C. Sales and D. Wohlleben, *Phys. Rev. Lett.* **35**, 1240 (1975).
- <sup>12</sup>P. F. de Chatel, J. Aarts, and J. C. P. Klaasse, *Commun. Phys.* **2**, 151 (1977).
- <sup>13</sup>E. Holland-Mortiz, M. Loewenhaupt, W. Schmatz, and D. K. Wohlleben, *Phys. Rev. Lett.* **38**, 984 (1977).
- <sup>14</sup>S. M. Shapiro, J. D. Axe, R. J. Birgeneau, J. M. Lawrence, and R. D. Parks, *Phys. Rev. B* **16**, 2225 (1977).
- <sup>15</sup>J. C. P. Klaasse, W. C. M. Mattens, F. R. de Boer, and P. F. de Chatel, *Physica (Utrecht) B* **86-88**, 234 (1977).
- <sup>16</sup>R. E. Majewski, A. S. Edelstein, A. T. Aldred, and A. E. Dwight, *J. Appl. Phys.* **49**, 2096 (1978).
- <sup>17</sup>(a) H. R. Krishna-murthy, K. G. Wilson, and J. W. Wilkins, in Ref. 1, p. 177; (b) *Phys. Rev. Lett.* **35**, 1101 (1975).
- <sup>18</sup>J. M. Lawrence and R. D. Parks, *J. Phys. (Paris)* **37**, C4-249 (1976); J. M. Lawrence, M. C. Croft, and R. D. Parks, Ref. 1, p. 35.
- <sup>19</sup>S. Doniach, Ref. 1, p. 169.
- <sup>20</sup>*X-Ray Diffraction Procedures*, H. P. Klug and L. E. Alexander (Wiley, New York, 1974), p. 222.
- <sup>21</sup>*Handbook of Chemistry and Physics*, 57th ed., edited by R. C. Weast (Chemical Rubber, Cleveland, 1976), p. E 195.
- <sup>22</sup>S. Foner, R. Doclo, and E. J. McNiff, Jr., *J. Appl. Phys.* **39**, 551 (1968).
- <sup>23</sup>E. W. Collings and R. D. Smith, *J. Less-Common Met.* **27**, 389 (1972).
- <sup>24</sup>F. D. M. Haldane, *Phys. Rev. Lett.* **40**, 417 (1978).
- <sup>25</sup>T. Murao and T. Matsubara, *Prog. Theor. Phys.* **18**, 215 (1957).
- <sup>26</sup>B. Barbara, J. X. Boucherle, J. L. Buevoz, M. F. Rossignol, and J. Schweizer, *Solid State Commun.* **24**, 481 (1977).
- <sup>27</sup>C. M. Varma, in Ref. 1, p. 201.